Use of a highly specific kinase inhibitor for rapid, simple and precise synchronization of *Plasmodium falciparum* and *Plasmodium knowlesi* asexual stage parasites

Margarida Ressurreição, James A. Thomas, Stephanie D. Nofal*, Christian Flueck, Robert W. Moon, David A. Baker† and Christiaan van Ooij†

Department of Infection Biology, London School of Hygiene & Tropical Medicine, Keppel Street, London WC1E 7HT, United Kingdom

ABSTRACT

During the course of the asexual erythrocytic stage of development, *Plasmodium* spp. parasites undergo a series of morphological changes and induce alterations in the host cell. At the end of this stage, the parasites exit the host cell, after which the progeny invade a new host cell. These processes are rapid and occur in a time-dependent manner. Of particular importance, egress and invasion of erythrocytes by the parasite are difficult to capture in an unsynchronized culture, or even a culture that has been synchronized to within hours. Therefore, precise synchronization of parasite cultures is of paramount importance for the investigation of these processes. Here we describe a method for synchronizing *Plasmodium falciparum* and *Plasmodium knowlesi* asexual blood stage parasites with ML10, a highly specific inhibitor of the cGMP-dependent protein kinase (PKG) that arrests parasite growth approximately 15 minutes prior to egress. This inhibitor allows parasite cultures to be synchronized to within minutes, with a simple wash step. Furthermore, we show that parasites remain viable for several hours after becoming arrested by the compound and that ML10 has advantages over the previously used PKG inhibitor Compound 2. Here, we demonstrate that ML10 is an invaluable tool for the study of *Plasmodium spp.* asexual blood stage biology and for the routine synchronization of *P. falciparum* and *P. knowlesi* cultures.

* current address: Signalling in Apicomplexan Parasites Laboratory, The Francis Crick Institute, London, UK

† for correspondence: David.Baker@lshtm.ac.uk, Christiaan.vanOoij@lshtm.ac.uk

INTRODUCTION

The asexual erythrocytic stage of the malaria parasite life cycle is marked by time-specific changes in parasite morphology and modifications to the host cell, driven by a just-in-time gene expression programme in the parasite [1-3]. Currently *P. falciparum*, *P. knowlesi* and *P. cynomolgi* are the only *Plasmodium spp*. that can be cultured *in vitro* [4-7], and to study these time-dependent changes in culture, the synchrony of the parasites needs to be artificially maintained. Whilst parasites remain synchronous *in vivo* [8-10], the absence of host interactions that regulate the synchrony of parasite development *in vitro* [8, 11] cause the parasites in the culture to become asynchronous – driven by small differences in the length of the replication cycle between individual parasites. This hinders the study of stage-specific processes, including host cell modification, formation of internal organelles, initiation of sexual differentiation, egress and invasion. Some of these processes are very rapid; egress, starting with rounding of the parasitophorous vacuole, followed by lysis of the parasitophorous vacuole membrane and finishing with the lysis of the erythrocyte plasma membrane, takes approximately 10 minutes [12-14], whereas merozoite invasion of fresh erythrocytes takes around 30 seconds for *P. falciparum* [15]. Hence, capturing these events and studying them biochemically requires parasites in culture to be tightly synchronized.

To overcome the problem of asynchrony in *in vitro* cultures, multiple methods of synchronization have been developed. Some of these methods interfere with the DNA synthesis pathway, arresting the parasites at the G1/S transition of the cell cycle. For example, the reversible DNA synthesis inhibitor aphidicolin has been used to arrest parasites prior to entry into S phase [16]. Similarly, treatment with DL-α-difluoromethylornithine depletes polyamines, inducing arrest at the G1/S transition [17, 18]. Addition of polyamines overcomes this arrest, allowing the parasites to enter the G1 phase of the cell cycle in a highly synchronized manner. This method has been used successfully to investigate the cell cycle in *P. falciparum* [18]. Other methods take advantage of the increased permeability of the plasma membrane of erythrocytes infected with mature stage parasites. Treatment of a culture with osmolytes such as D-sorbitol and D-mannitol lyses erythrocytes infected with trophozoite- and schizont-stage parasites, without affecting erythrocytes infected with ring-stage parasites [19]. This has the disadvantage that the developmental stage of the remaining parasites can still vary widely, as even after 18 hours post-invasion (in the case of *P. falciparum*) lysis with these osmolytes is inefficient. Infected erythrocytes containing late-stage *P. knowlesi* parasites can be selectively lysed using guanidine hydrochloride, as they are less sensitive to sorbitol treatments [20]. Similarly, treatment with the pore-forming toxin Streptolysin O has been described as a method to selectively remove erythrocytes infected with late-stage parasites [21]. Furthermore, a microfluidics device has been developed for the enrichment of ring-stage parasites [22]. Other more commonly used methods take advantage of the decreased density of infected erythrocytes containing more mature stages, such as density centrifugation using a Percoll or Nycodenz cushion, to separate erythrocytes infected with later stage parasites from erythrocytes infected with ring-stage parasites and uninfected erythrocytes [23-26]. These schizonts can then be allowed to invade fresh erythrocytes for a limited time followed by removal of the remaining late-stage parasites with a second cushion flotation and/or a treatment with D-sorbitol. This enables establishment of culture with a known synchronicity [27, 28]. However, to obtain a useful parasitemia, an invasion period of several hours is usually required, which is often too long for the precise investigation of rapid processes such as egress and invasion.

Other methods take advantage of the paramagnetic properties of the hemozoin crystal that is formed during the breakdown of hemoglobin to separate erythrocytes infected with late-stage parasites from uninfected erythrocytes and erythrocytes infected with younger parasites [29-31]. Parasites that have started producing hemozoin will adhere to the matrix of a magnetic-activated cell sorting (MACS) column while the younger parasites and uninfected erythrocytes pass through. This method yields a very high percentage of infected cells, but as the formation of the paramagnetic hemozoin crystal starts relatively early in the erythrocytic cycle, the isolated parasites can vary in age by many hours.

To provide higher degrees of synchrony, various other methods have been developed. For instance, by overlaying schizont-infected erythrocytes immobilized using concanavalin A with uninfected erythrocytes, newly infected erythrocytes can be harvested from the supernatant [32], thereby allowing parasites to be synchronized to within a thirty-minute window.

The method of synchronization with the best temporal resolution is the filtration method. Here, parasite egress is blocked with the irreversible cysteine protease inhibitor E64, followed by mechanical lysis of infected erythrocytes by filtration. In the case of *P. falciparum*, parasites are passed through a 1.5 μm filter, whereas for *P. knowlesi* double filtration through a 3 μm filter followed by 2 μm filter is applied, resulting in a nearly instantaneous release of infectious merozoites [33-35]. This method provides a resolution of invasion of seconds to minutes and has provided important insights [36]. However, the proportion of viable merozoites produced by this method is highly variable and can be quite low. So whilst well-suited for comparing the effect of treatments on a single parasite strain (e.g. drug treatments), comparisons between different parasite strains are challenging (such as comparing mutant and wild-type parasites). This precludes its use for larger-scale investigations and assays and would be cumbersome to apply to routine synchronization of parasite cultures.

To overcome these drawbacks, chemical inhibition of cyclic GMP (cGMP)-dependent protein kinase (PKG) has been used to synchronize parasites. Activation of PKG initiates a signaling cascade that promotes the lysis of the parasitophorous vacuole membrane and the erythrocyte membrane; inhibition of this kinase arrests the parasites at a step immediately prior to the initiation of egress [37-40]. Subsequent removal of reversible PKG inhibitors leads to rapid release of merozoites. One such inhibitor, an imidazopyridine referred to as Compound 2 (4-[7-[(dimethylamino)methyl]-2-(4-fluorophenyl)imidazo[1,2-α]pyridine-3-yl]pyrimidin-2-amine) [41], has been applied to the study of egress and invasion. The timed release of a synchronized culture of parasites allows these rapid events to be visualized which are normally extremely difficult to observe, even in a population where the window of synchronization is hours [13, 14, 38, 42-45]. However, a detailed description of the use of PKG inhibitors has not been published. Recently a highly specific and potent derivative of Compound 2, referred to as ML10, with a single digit nM EC_{50} and an approximately 75-fold higher specificity has been described [46]. To demonstrate that ML10 is a valuable tool for the synchronization of *Plasmodium* spp. parasites, we determined a number of important parameters for the use of this compound.

141
142 **RESULTS**
143 **Working concentration of ML10 for *P. falciparum* and *P. knowlesi***
144 To develop ML10 as a reagent for the synchronization of malaria parasites, we first derived
145 an optimal working concentration. The EC_{50} of ML10 on the *P. falciparum* strain 3D7 was
146 determined using a standard 72-hour SYBR Green growth inhibition assay, starting with
147 young trophozoite-stage parasites [47]. With this assay, an EC_{50} of 4.2 nM (±SD 2.7 nM) was
148 obtained (Figure 1A, Table 1, Supp. Figure 1A), very similar to the EC_{50} of 2.1 nM (±SD 0.2
149 nM) determined previously using the hypoxanthine incorporation assay [46]. The EC_{50} of
150 Compound 2 in the same SYBR Green 72-hour growth inhibition assay was 100 nM (±SD 35
151 nM), also similar to previously published values using the hypoxanthine incorporation assay
152 (Figure 1B, Supp. Figure 1B) [46]. To verify the specificity of the inhibitors for PKG in the
153 SYBR Green assay, we determined in parallel the EC_{50} for a 3D7-derived transgenic line that
154 harbors a gatekeeper mutation (T618Q) in the PKG sequence [40, 46]. In this mutant, access
155 to the ATP-binding pocket is blocked, preventing binding of ATP-competitive PKG inhibitors
156 that utilise the gatekeeper pocket, including ML10, Compound 2 and Compound 1,
157 however, this mutation has no detectable effect on the endogenous activity of PKG or
158 parasite growth [41, 46, 48]. The EC_{50} values of ML10 and Compound 2 in this strain were
159 several orders of magnitude higher than that of 3D7 (Figures 1C and 1D), confirming that
160 ML10 is indeed a highly specific inhibitor of PKG, as previously described [46]. As the results
161 using the 72-hour SYBR Green growth inhibition assay closely replicated the data previously
162 obtained with the hypoxanthine incorporation assay, it was deemed suitable for further
163 investigation of ML10. Based on these results, we set the working concentration of ML10 for
164 subsequent experiments at 25 nM, a concentration approximately six-fold higher than the
165 EC_{50} for wild type parasites, but that had no effect on the gatekeeper mutant parasites.
166 From this we conclude that at this concentration, ML10 does not affect any essential target
167 other than PKG.
168 To investigate whether the 25 nM working concentration used for 3D7 would be
169 widely applicable to other *P. falciparum* isolates, we determined the EC_{50} of ML10 in three
170 additional *P. falciparum* laboratory isolates from different parts of the world and with
171 different drug resistance phenotypes [49]: Dd2 (originally from Southeast Asia, has
172 increased resistance to chloroquine, cycloguanil and pyrimethamine), HB3 (originally from
173 Honduras, has increased resistance to cycloguanil and pyrimethamine) and NF54 (isolated
174 from a case of 'airport malaria'; this strain has similarities to African parasite strains [50])
175 from which 3D7 is derived. The EC_{50} values obtained for these strains were 5.14 nM (±SD 1.5
176 nM) for Dd2, 4.86 nM (±SD 2.9 nM) for HB3 and 6.87 nM (±SD 2.0 nM) for NF54 (Figures 2A,
177 2B and 2C, Table 1, Supp. Figure 1A). The EC_{50} of Compound 2 in these strains was
178 determined to be 150 nM (±SD 46 nM) for Dd2, 104 nM (±SD 36 nM) for HB3 and 130 nM
179 (±SD 12 nM) for NF54 (Figures 2D, 2E and 2F, Table 1, Supp. Figure 1B). Hence, ML10 and
180 Compound 2 affect these distinct *P. falciparum* laboratory isolates similarly and therefore
181 the 25 nM working concentration is likely to be effective for many, if not all, *P. falciparum*
182 isolates.
183 Next, we established the EC_{50} of ML10 for *P. knowlesi*, the only other human malaria
184 species that can be cultured *in vitro* in human red blood cells [5, 6], using the same SYBR
185 Green growth assay. Surprisingly, the EC_{50} of ML10 for this species was determined to be
186 43.8 nM (±SD 5.6 nM) (Figure 3A), over ten-fold higher than for *P. falciparum*. Whereas *P.*
187 *falciparum* is grown in medium containing only 0.5% AlbuMax, *P. knowlesi* is cultured *in*

188 *vitro* in a high-serum medium containing both 10% horse serum and 0.5% AlbuMax, and this
189 additional protein binding content is known to increase EC_{50} values owing to the binding of
190 compounds to serum components [51]. To determine if this was the case for ML10, we
191 measured the EC_{50} of ML10 for *P. falciparum* 3D7 grown in the horse serum-containing
192 medium used to culture *P. knowlesi*. This revealed that the addition of serum increases the
193 EC_{50} of ML10 in *P. falciparum* 3D7 parasites to 17 nM (Figures 3B, Table 1, Supp. Figure 1B),
194 approximately four-fold higher than when grown without serum – indicating the serum
195 content of the medium accounted for the majority of the differential susceptibility. We
196 therefore tested whether a concentration of 150 nM ML10 could arrest a *P. knowlesi* culture
197 without affecting the viability of the parasites. Treatment of a *P. knowlesi* culture did indeed
198 arrest parasites at the end of the cycle (Figure 3C). When ML10 was removed when ring-
199 stage parasites were detected in the DMSO-treated control samples (approximately two
200 hours after the addition of ML10), the parasites were able to egress and invade new
201 erythrocytes, demonstrating that they remained viable after ML10 treatment (Figure 3C). As
202 *P. falciparum* parasites are also often cultured in the presence of human serum, we further
203 tested whether 25 nM, 50 nM or 75 nM ML10 would be an effective concentration to arrest
204 *P. falciparum* grown in the presence of human serum. We found that when cultured in
205 either the presence of 10% human serum (Figure 3D) or 5% human serum in addition to
206 0.5% AlbuMax (Figure 3F), 25 nM ML10 did not effectively block progression of the
207 parasites, whereas 50 nM and 75 nM ML10 did. Hence, using a concentration of 50 nM
208 ML10 in cultures containing human serum is sufficient to arrest parasites (Table 1).
209
210 **Schizont rupture arrested with ML10**
211 As ML10 reversibly blocks the intra-erythrocytic parasite at a stage immediately prior to the
212 onset of egress, it is an ideal reagent to synchronize egress and the subsequent invasion of
213 merozoites to obtain highly synchronized cultures. However, synchronization of an
214 asynchronous parasite culture requires that the most mature parasites be held in an
215 arrested state for an extended time until the younger parasites reach the same arrested
216 state. To determine the length of time that arrested parasites remain viable, we tightly
217 synchronized a 3D7 culture with two sequential flotations on a Percoll cushion.
218 Approximately 45 hours later, when rings were detected in the culture, schizonts were
219 isolated and mixed with uninfected erythrocytes to give a final parasitemia of ~1%. This
220 culture was split into three flasks, to which either DMSO, 25 nM ML10 or 1.5 μM Compound
221 2 was added. These cultures were then incubated at 37˚C for 1-12 h. At the end of the
222 incubation period, the parasites were pelleted and resuspended in fresh medium without
223 compound, allowing viable parasites to egress and invade fresh erythrocytes. The resulting
224 parasitemia serves as a measure of the survival of the schizonts during the incubation in the
225 presence of ML10 and Compound 2. This revealed that incubation in the presence of ML10
226 for up to three hours did not affect the viability of the parasites and that the effect of ML10
227 on parasite viability after four hours was generally small (Figure 4A). However, a noticeable
228 decline in viability was detected after six hours, with further declines as the length of the
229 incubation increased. As the viability of the parasites decreased, they took on a bloated
230 appearance in Giemsa-stained blood films, in contrast to the healthy appearance of
231 parasites seen in the samples treated for shorter periods (Figure 4B). Interestingly, the
232 survival of parasites incubated in the presence of Compound 2 was consistently lower
233 (Figure 4A). Nonetheless, the viability of parasites incubated in the presence of Compound 2
234 showed a similar decrease in viability over time as those incubated with ML10: decreasing

after four hours in the presence of the compound, with larger decreases starting after six hours on incubation. The higher level of survival of parasites in the presence of ML10 as compared to Compound 2 indicates that this compound may be a superior choice for the synchronization of parasites.

Timing of egress after removal of ML10 and synchronicity of resulting cultures

Induction of PKG activity initiates a cascade of downstream events that ultimately results in egress [37, 38, 40], causing a delay between the initiation of PKG activity after the removal of ML10 and egress. Video microscopy was used to monitor egress of closely synchronized late schizonts arrested with ML10 or Compound 2 and following the removal of the compounds. When ML10 was tested, on average the first parasites began to egress 17 mins 18 s (±SD 3 min 38 s) after ML10 washout and many of the parasites that egressed in the course of the imaging were detected within an 11 minute window (±SD 4 min 16 s) (Supp. video 1 and Supp. Figure 2). When Compound 2 was tested in this assay, release of parasites was detected in a similar timeframe, with the first parasites egressing on average 16 mins 48 s (±SD 5 min 7 s) after compound removal and the remaining parasites that egressed in the course of the imaging were released within a 13 minute and 50 s window (±SD 2 min 45 s SD) (Supp. video 2 and Supp. Figure 2). This is comparable to previously reported timings of parasite release following the removal of Compound 2 [14, 38, 42].

The results of the video microscopy indicated that the burst of merozoite release was very synchronous, although not all parasites egressed during the imaging period. This may reflect that these parasites had not yet matured to the stage where they were blocked by either compound at the time it was removed or that a fraction.

To determine the synchronicity of invasion after removal of ML10, we measured the appearance of ring-stage parasites in the culture by flow cytometry at 10-min intervals after the removal of ML10 or Compound 2. Most egressed parasites were detected 20 min after the removal of the compound, with only very small increases afterwards, indicating that egress of parasites after removal of the compounds occurs in a narrow time window and results in a highly synchronous culture (Figures 5A and 5B). Whereas it was difficult to distinguish attached from invaded merozoites at the 20-minute time point, at the 30-minute time point, the parasites had progressed to the typical ring-shaped morphology of very young parasites, indicating that they had entered the erythrocyte. Interestingly, treatment with Compound 2 resulted in fewer ring-stage parasites compared to treatment with ML10, similar to what was observed when parasites were incubated in ML10 or Compound 2 for extended periods of time (Figure 4), again potentially indicating that there are off-target effects of Compound 2, although the timing of the appearance of new rings and the synchrony were very similar between the two compounds.

Development of parasites through the erythrocytic cycle in the presence of ML10

All of the above experiments were performed by adding ML10 to mature schizonts, either in culture or purified by flotation on a Percoll cushion. However, for the continued maintenance of a synchronous culture, it would be beneficial if the compound could be added at any stage of the cycle. To test if ML10 affects any other part of the intraerythrocytic cycle, we added either DMSO or ML10 to a culture of ring-stage parasites that had invaded within the previous two hours. We subsequently monitored the development of the parasites by Giemsa staining and by measuring the increase in DNA content of the parasites by flow cytometry. This revealed no obvious difference between

282 the DMSO-treated and ML10-treated parasites in their progression through the
283 intraerythrocytic cycle (Figures 6A). To examine if viable merozoites were produced by
284 parasites that had developed for the entire cycle in the presence of ML10, DMSO and ML10
285 were removed from the cultures three hours after ring-stage parasites were first detected in
286 the DMSO-treated culture. At this time, the parasites in the ML10-treated culture had been
287 blocked for up to three hours by the compound and hence had completed the entire intra-
288 erythrocytic cycle in the presence of the compound. When the parasitemia of the cultures in
289 the next cycle was determined, no significant difference was detected, indicating that ML10
290 does not affect the growth of the parasites and the production of viable merozoites even
291 when the compound is present throughout the entire intra-erythrocytic cycle (Figure 6B).
292 To determine if treatment with ML10 can have subtle effects on the parasites if used
293 over prolonged periods, we tested the effect of continuous treatment with ML10 on the
294 growth of the T618Q strain and 3D7 over several cycles. The T618Q strain was not affected
295 by the presence of ML10, as indicated by the identical growth rate in the presence or
296 absence of ML10, whereas the 3D7 strain grew only in the absence of ML10 (Figure 6C). This
297 further shows that at the concentration used (25 nM) the only essential molecule in the
298 parasite affected by ML10 is PKG.
299
300 **DISCUSSION**
301 The data presented here provide the first in-depth analysis of the use of PKG inhibitors as
302 tools to synchronise and study the intra-erythrocytic cycle of *Plasmodium* spp. parasites. We
303 show that the PKG inhibitor ML10, a derivative of the previously used imidazopyridine PKG
304 inhibitor Compound 2 [46], reversibly arrests *P. falciparum* and *P. knowlesi* at a very late
305 schizont stage at low nanomolar concentrations. Whereas we detected no significant
306 difference in the EC_{50} of ML10 among four different *P. falciparum* laboratory isolates, the
307 EC_{50} of ML10 was markedly influenced by the supplement used in the medium; human and
308 horse serum increase the EC_{50} compared with medium containing AlbuMax, likely owing to
309 binding of the compound to serum components. The EC_{50} for *P. knowlesi* was found to be
310 higher than that for *P. falciparum*, even when *P. falciparum* was grown in the presence of
311 serum, indicating a difference in biology that may make it slightly less susceptible to PKG
312 inhibition. This is similar to previous findings, which established that the EC_{50} values of
313 certain anti-malarials are higher for *P. knowlesi* than for *P. falciparum* [51, 52]. Nonetheless,
314 we have been able to successfully calibrate concentrations that are effective in the two
315 species and in several media formulations (Table 1).
316 Removal of ML10 leads to a highly synchronous burst of egress and subsequent
317 invasion, as a large fraction of the parasites released after the removal of the compound
318 had invaded within a ten-minute window. By preventing further invasion through the
319 addition of compounds known to inhibit invasion, such as heparin [53], a culture could be
320 established in which the parasites are matched in age to within minutes.
321 In contrast to other methods for synchronizing *Plasmodium* cultures, which can be
322 labour-intensive or require specialized equipment, synchronizing cultures with ML10 is fast
323 and simple. Removal of the compound from an arrested culture with a single wash step
324 leads to egress of the arrested parasites and invasion of erythrocytes within 20 minutes. As
325 parasites arrested by ML10 retain their viability for several hours, a semi-synchronized
326 parasite culture can be treated with ML10 for an extended period to allow a subset of
327 parasites to reach the point in the cycle where they become arrested. Subsequent removal
328 of the compound will then cause a proportion of parasites to undergo egress and invade

329 fresh erythrocytes in a very short time span. Parasites that have not reached the point of
330 ML10 arrest, and hence have not yet egressed, can then be removed on a Percoll cushion or
331 by lysis with 5% D-sorbitol, thereby establishing a highly synchronized culture. As ML10 does
332 not affect any essential parasite proteins other than PKG, synchronicity in the culture can
333 then be maintained simply by adding ML10 at any stage of the asexual cycle and removing
334 the compound when the parasites become arrested prior to the initiation of egress. In our
335 experience, simply replacing the medium in a culture flask with fresh medium is sufficient to
336 lower the concentration of ML10 to below its effective concentration and allow egress and
337 subsequent invasion. Hence, addition of ML10 provides a very simple method for the
338 maintaince of synchronicity of parasite cultures over many cycles.
339 Synchronized cultures are of great value in the study of many processes in the
340 asexual cycle and the ability to synchronize egress and invasion to within minutes will allow
341 the investigation of these rapid processes on different scales, allowing for a wide range of
342 studies, including large-scale biochemical investigation of proteins involved, such as the
343 proteolysis of MSP1 and AMA1 proteins [54-56]. Furthermore, as it makes timing of egress
344 and invasion very predictable, this method will greatly aid the imaging of egress and
345 invasion by video microscopy. In addition, a culture of such tightly synchronized parasites
346 will be of great benefit for the study of very early ring-stage parasites; parasites at this stage
347 undergo very rapid changes [57, 58] that are difficult to capture on a population level in a
348 culture in age by hours. An additional application of the very tight synchronization is the
349 preparation of parasites for schizont-stage transfection, which requires extremely
350 synchronized parasites [6, 59]. Compound 2 has been used previously to aid synchronization
351 of *P. knowlesi* for transfection [44]. Furthermore, ML10 has recently been used to block the
352 proliferation of asexual stages in a *P. falciparum* culture induced to form gametocytes [60].
353 Of the PKG inhibitors used for synchronization of parasite cultures, Compound 2 has
354 been the most commonly used [14, 38, 42, 44, 45, 54, 55, 61]. However, the results shown
355 here indicate that ML10 has advantages over Compound 2. Owing to its potency, ML10 can
356 be used at extremely low concentrations (25 nM in the case of *P. falciparum* cultured in
357 AlbuMax, compared to a working concentration of 1 μM in the case of Compound 2),
358 allowing the concentration of the DMSO solvent, which is used to dissolve both ML10 and
359 Compound 2, to remain very low as well; high concentrations of DMSO can have deleterious
360 effects on eukaryotic cells [62, 63]. The low working concentration of ML10 also ensures
361 that stock solutions are not rapidly depleted, allowing routine synchronization of large-scale
362 cultures, and the higher specific activity of ML10 compared to that of Compound 2
363 additionally reduces the likelihood that any phenotype detected is the result of off-target
364 effect of the compound. Furthermore, we consistently saw a small but noticable decrease in
365 the viability of the parasites treated with Compound 2, even after short incubations with the
366 compound (Figures 4 and 5). This loss of viability was not detected in parasites treated with
367 ML10, indicating that Compound 2 may have additional off-target effects on the parasites or
368 is not washed away as readily as ML10.
369 In conclusion, we believe that ML10 will be a very valuable tool for the investigation
370 of the asexual erythrocytic stage of the lifecycle of *Plasmodium spp.* The compound is
371 available from LifeArc.
372
373 **MATERIAL AND METHODS**
374 *Parasite culture*

375 Unless otherwise stated, all *P. falciparum* experiments were performed with the 3D7 strain
376 and all *P. knowlesi* experiments were performed with the A1-H.1 strain [6]. Both species
377 were maintained in RPMI-1640 medium (Life Technologies) supplemented with additional
378 glucose, 0.5% AlbuMax type II (Gibco), 50 µM hypoxanthine and 2 mM L-glutamine
379 (complete medium) at 2-3% hematocrit at 37˚C. In the case of *P. knowlesi*, this medium was
380 further supplemented with 10% (v/v) horse serum (PAN Biotech; [64]). *P. falciparum* was
381 maintained in the presence of 5% CO_2, whereas *P. knowlesi* was maintained in the presence
382 of 96% N_2, 1% O_2, 3% CO_2. Human erythrocytes were obtained from the National Blood
383 Transfusion Service, UK.
384
385 *Measurement of EC_{50} by SYBR Green assay*
386 To assess the ML10 concentration required to block *P. falciparum* and *P. knowlesi* egress
387 and compare this to Compound 2, an *in vitro* 72 h SYBR Green growth inhibition assay was
388 adapted from Smilkstein et al. and van Schalkwyk et al. [47, 51]. A starting culture consisting
389 of synchronous young trophozoite *P. falciparum* or *P. knowlesi* parasites was adjusted to 2%
390 parasitaemia and 2% haematocrit. Starting ML10 and Compound 2 concentrations were 2-
391 fold serially diluted in triplicate in 50 µl complete medium in a 96-well plate to provide a
392 concentration range of 400 nM to 0.024 nM for ML10 and 50 µM to 3 nM for Compound 2.
393 Subsequently, 50 µl of culture was added to each well, to produce a final parasitemia and
394 hematocrit of 1%. The highest DMSO concentration present in the assay was 0.05%. The 96-
395 well culture plates were maintained at 37˚C for 72 h in the case of *P. falciparum* and 48 h in
396 the case of *P. knowlesi* and subsequently frozen. For lysis and fluorescence analysis, plates
397 were thawed at 37˚C and 100 µl of lysis buffer (20 mM Tris pH 7.5, 5 mM EDTA, 0.008%
398 Saponin and 0.08% Triton X-100 in distilled H_2O) complemented with SYBR Green I Nucleic
399 Acid Stain at a concentration of 2x (from a 10,000 x stock; Fisher Scientific) was added and
400 incubated in the dark at room temperature for 1 h after thorough mixing. Subsequently,
401 relative fluorescent units were recorded using a Spectramax 3 spectrophotometer with
402 excitation and emission settings at 485 and 535 nm, respectively. The data were obtained in
403 relative fluorescent units and fitted to a dose-response curve (GraphPad Prism 8 software).
404 The EC_{50} (here defined as the drug concentration that gives half the maximal response of
405 egress arrest) was determined by dose-response non-linear regression analysis of the log
406 dose-response curves.
407 To determine if 150 nM ML10 was an appropriate working concentration for *P.*
408 *knowlesi*, late stage parasites were purified on a cushion of 55% Nycodenz as described
409 previously [6], washed in RPMI 1640 and allowed to egress and infect fresh erythrocytes in
410 complete *P. knowlesi* medium [6] with agitation for 1 h before lysis of remaining late stage
411 parasites in 140 mM guanidine hydrochloride, 20mM HEPES, pH7.4 as previously described
412 [20]. Late stage *P. knowlesi* parasites were then purified on 55% Nycodenz 72 h later.
413 Parasites were then added to a suspension of fresh erythrocytes at ~2 % haematocrit in
414 complete *P. knowlesi* medium to achieve a parasitaemia of ~2 %. Negative control cultures
415 containing only erythrocytes were included in order to subtract background 'parasitaemia'
416 counts. ML10 was then added to a final concentration of 150 nM to relevant cultures,
417 whereas an enquivalent volume of DMSO was added to the untreated sample, and cultures
418 incubated at 37° C for 2 h, at which time the presence of ring-stage parasites was verified by
419 Giemsa-stained thin smears in the cultures lacking ML10. Cells were then pelleted in a
420 microfuge at ~2800 x g (MiniSpin®, Eppendorf) for 1 min before washing once with
421 complete medium in the presence or absence of ML10 before suspending cells in complete

422 medium for overnight incubation at 37° C in the presence or absence of ML10. Samples
423 were set up in triplicate, with separate addition of ML10. Aliquots of the samples were fixed
424 after the initial addition of ML10 to determine the starting parasitemia and again 17 h after
425 washing. Fixation was performed in 0.02 % glutaraldehyde for 30 min at room temperature
426 before storage at 4° C until required. SYBR Green I (Invitrogen) was added to aliquots of
427 fixed parasites according to manufacturer's instructions (10,000 x dilution) and parasites
428 stained for 30 min at room temperature before dilution of fixed cells in 5 x volumes of PBS
429 before parasitaemia was determined by flow cytometry using an Attune NxT.
430 To determine how the presence of serum in culture might affect the efficiency of
431 ML10 to arrest egress, a synchronous culture of late-stage 3D7 parasites maintained in
432 RPMI-1640 containing 0.5% AlbuMax was pelleted and resuspended in RPMI-1640
433 containing 10% human serum (without AlbuMax). The parasitemia was adjusted to 1% and
434 the parasites were then added to wells of a 48-well plate and ML10 was added to a final
435 concentration of 0-75 nM. Aliquots were removed and fixed to determine the starting
436 parasitemia. The following day aliquots were removed, fixed and stained with 4.0%
437 formaldehyde, 0.1% glutaraldehyde and SYBR Green I to determine the parasitemia of the
438 culture by flow cytometry, as a measure of progression to the next cycle. In parallel, a
439 culture of 3D7 that had been maintained in RPMI-1640 containing 0.5% AlbuMax and 5%
440 human serum was treated similarly to determine the effect of human serum on the EC_{50} of
441 ML10.
442
443 *Time-lapse video microscopy*
444 To determine the period of time required for arrested schizonts to rupture and merozoites
445 to egress after removal of ML10 or Compound 2, parasite cultures were maintained and
446 assays were performed as follows. Parasites were synchronised by allowing schizonts
447 recovered from an initial Percoll flotation to invade fresh erythrocytes for 90 minutes. The
448 culture was subsquently treated with a second Percoll flotation and 5% D-sorbitol for 20
449 minutes at 37˚C to retain only newly formed rings. The tightly synchronised culture of 3D7
450 parasites was then maintained as standard until schizonts were detected in Giemsa smears
451 (approximately 45 hours after D-sorbitol treatment). The developed schizonts were then
452 purified on a Percoll cushion, washed twice with medium and split equally into three
453 different microcentrifuge tubes for a final volume of 1 ml medium in the presence of
454 medium only (to monitor schizont development and rupture), 30 nM of ML10 or 1 µM of
455 Compound 2 at 37˚C. When late schizonts were detected and ring-stage parasites started to
456 appear in the non-treated sample (approximately two to three hours later) the compound-
457 arrested parasites were considered ready for washout. Meanwhile, untreated glass viewing
458 chambers [38], medium and Lab Armor™ Beads were maintained at 37˚C. When ready,
459 parasites were spun down at 2500xg for 15 seconds, the supernatant removed and replaced
460 with 500 µl of pre-warmed complete medium. Parasites were then added onto the pre-
461 warmed viewing chambers and transported in a box with pre-warmed Lab Armor™ Beads.
462 Time-lapse DIC imaging was initiated 10 minutes after addition of wash medium. Images
463 were taken on a Nikon Ti Eclipse microscope fitted with OKO-lab environmental controls
464 and a Hamamatsu C11440 digital camera and Nikon N Plan Apo λ 100x/1.45NA oil
465 immersion objective. Images were taken at 5 s intervals over a total of 30 min, then
466 exported as TIFFs or AVI, annotated and saved as mp4 files using Nikon NIS-Elements
467 software. Videos for both ML10 and Compound 2 were in all cases taken from the same day
468 experiment. A total of 3 independent experiments were quantified (Supp. Figure 2).

469 Quantification was performed using ImageJ and manually annotating in a pairwise manner
470 the time taken for the first schizonts to egress and then the time for most schizonts in view
471 to egress.
472
473 *Monitoring ring formation after removal of ML10 or Compound 2*
474 To detect the formation of ring-stage parasites after release from ML10 or Compound 2 the
475 following assay was designed. Tightly synchronised Percoll-purified schizonts were split
476 equally into 1 mL of medium containing either 30 nM ML10 or 1 µM Compound 2 and
477 maintained at 37˚C for a maximum of 4 h, at which time the compound was removed by
478 briefly centrifuging the cultures, aspirating the supernatant and resuspending the parasites
479 in 1 ml of prewarmed medium at 3% haematocrit. Immediately, two 50 µl replicates were
480 removed and fixed into 50 µl 2X fixative for a final concentration of 4% formaldehyde,
481 0.01% glutaraldehyde and 1X SYBR Green I and an additional 30 µl aliquot was removed for
482 Giemsa staining; this was considered the starting time point (T=0). The remaining culture
483 was left shaking at 37˚C and samples were acquired as before after 10, 20, 30, 60 and 120
484 minutes. Images of Giemsa-stained smears were captured using an Olympus BX51
485 microscope equipped with an 100x oil objective and an Olympus SC30 camera. Comparative
486 measurements of ring formation were obtained using an Attune NxT Flow Cytometer and
487 analysed with Attune NxT Flow Cytometer software (ThermoFisher Scientific). SYBR Green I-
488 positive erythrocytes were gated from a total of 200,000 singlet events and a gating strategy
489 based on the area of SYBR Green I-positive signal was used to differentiate the schizont-
490 stage parasites from ring-stage parasites (Supp. Figure 2). The percentage of ring-stage
491 parasites was calculated from the total parasitaemia, i.e. all parasitized cells with a positive
492 SYBR Green I value.
493
494 *Survival of arrested* P. falciparum *parasites*
495 To determine how long *P. falciparum* parasites survive when arrested in ML10, a parasite
496 culture was tightly synchronized using successive Percoll flotations less than two hours
497 apart, followed by treatment with 5% D-sorbitol and subsequently incubated at 37˚C. When
498 ring-stage parasites were detected in the culture approximately 45 h later, indicating
499 initiation of progression of the parasites to the subsequent cycle, schizont-stage parasites
500 were isolated on a Percoll cushion. These schizonts were mixed with uninfected
501 erythrocytes at a parasitemia of approximately 1%. ML10, Compound 2 or DMSO was
502 immediately added to the culture to produce final concentrations of 25 nM, 1.5 µM or
503 0.025% (v/v) (matching the DMSO concentration of the ML10 sample), respectively. To
504 remove the inhibitor, four 250 µl aliquots of the culture were removed, centrifuged briefly
505 to pellet the erythrocytes. The supernatant was removed and the erythrocytes were
506 resuspended in medium lacking inhibitor or DMSO. The resuspended parasites were
507 subsequently placed in a well of a 48-well plate and incubated until the end of the cycle,
508 when 50 µl of the culture was mixed with fixative solution containing 8% formaldehyde,
509 0.2% glutaraldehyde and 1X SYBR Green I in PBS. Fixed parasites were stored at 4˚C and the
510 parasitemia was determined using flow cytometry on an Attune NxT cytometer using Attune
511 NxT Flow Cytometer software.
512
513 *Growth of* P. falciparum *in the presence of ML10*
514 To determine the effects of ML10 on the growth of the parasites during the entire asexual
515 erythrocytic cycle, a parasite culture was synchronized to within two hours using successive

516 Percoll cushions and sorbitol treatment. The culture was split and either 25 nM ML10 or an
517 equivalent volume of DMSO was then added. Synthesis of DNA was monitored by flow
518 cyctometry using parasites that had been fixed with 4% formaldehyde and 0.1%
519 glutaraldehyde and stained with SYBR Green I at various time points over two erythrocytic
520 cycles. To determine if ML10-treated parasites produced invasive merozoites, ML10 and
521 DMSO were removed 47 hours after the start of the erythrocytic cycle, three hours after the
522 first appearance of rings in the DMSO-treated samples to ensure that the ML10 treatment
523 covered the entire intra-erythrocytic cycle, from the earliest ring stage to the block of PKG
524 activity.
525 To investigate the effect of ML10 upon continued exposure of the parasites to the
526 compound, the growth of *P. falciparum* T618Q parasites in the presence of ML10 or DMSO
527 over several erythrocytic cycles was measured. Cultures of *P. falciparum* T618Q and 3D7
528 parasites were adjusted to a parasitemia of ~0.1%, DMSO or ML10 were added to 0.025%
529 (v/v) and 25 nM, respectively (ensuring an equal concentration of DMSO in each sample)
530 and growth was subsequently measured over four cycles. Starting four days after the
531 addition of the compound, the medium was replaced with fresh medium containing DMSO
532 or ML10 daily. The parasitemia was measured by flow cytometry as described above.
533
534 *Statistical analysis*
535 Statiscal analyses were performed using GraphPad Prism 8 software and significance is
536 represented as *** $p \leq 0.001$, ** $p \leq 0.01$ and * $p \leq 0.05$. The different statistical analyses
537 applied in this study are described in the respective figure legends, when applicable.
538
539
540 **Acknowledgments**
541 We thank Avnish Patel for constructive feedback on experimental design, Donelly van
542 Schalkwyk for providing Dd2 parasites, Julian Muwanguzi-Karugaba for providing HB3
543 parasites and Michael Delves for providing human serum. This work was supported by
544 Medical Reseach Council Career Development Awards MR/R008485/1 (CvO) and
545 MR/M021157/1 (RWM) (jointly funded by the UK MRC and the UK Department for
546 International Development), Wellcome Trust grant 106240/Z/14/Z (DAB), British Biological
547 Sciences Research Council grant BB/M009513/1 (SDN) and Wellcome Trust Sir Henry
548 Wellcome fellowship 210861/Z/18/Z (JAT).

549
550 **Table 1**
551 EC50 of ML10 for different *Plasmodium* species grown in RPMI-1640 containing various
552 medium supplements.
553

Species	Strain	Medium supplement	EC50 ± SD	Working concentration
Plasmodium falciparum	3D7	AlbuMax	4.2 ± 2.7 nM	25 nM
Plasmodium falciparum	3D7	AlbuMax, 10% HoS	17.9 ± 3.3 nM	50 nM
Plasmodium falciparum	HB3	AlbuMax	4.9 ± 2.9 nM	25 nM
Plasmodium falciparum	Dd2	AlbuMax	5.1 ± 1.5 nM	25 nM
Plasmodium falciparum	NF54	AlbuMax	6.9 ± 2.0 nM	25 nM
Plasmodium knowlesi	A1-H.1	AlbuMax, 10% HoS	43.8 ± 5.6 nM	150 nM

561

562 **FIGURE LEGENDS**
563
564 **Figure 1. Dose-response curves of ML10 and Compound 2 for *P. falciparum* 3D7 and T618Q**
565 **parasites.**
566 *P. falciparum* 3D7 parasites (**A** and **B**) and T618Q parasites that harbor a gatekeeper
567 mutation in the gene encoding PKG (**C** and **D**) were cultured in the presence of decreasing
568 concentrations of ML10 (**A** and **C**) or Compound 2 (**B** and **D**). Parasite growth was
569 determined using a 72-hour SYBR Green assay and the EC_{50} value for the compounds was
570 calculated for each strain from the resulting dose-response curve. Shown are representative
571 graphs from one of five replicates. For EC_{50} values of all five experiments, see Supp. Figure 1;
572 for the average EC_{50} values, see Table 1. For both compounds, the difference between the
573 EC_{50} for 3D7 and the T618Q parasites was statistically significant by an unpaired t-test, in
574 both cases, $p \leq 0.001$.
575
576 **Figure 2. Dose-response curves of *P. falciparum* strains Dd2, HB3 and NF54 cultured in the**
577 **presence of ML10 or Compound 2.** *P. falciparum* strains Dd2, HB3 and NF54 were cultured
578 in the presence of decreasing concentrations of ML10 (**A**-**C**) or Compound 2 (**D**-**F**) for 72
579 hours and growth was determined by staining with SYBR Green. The resulting dose-
580 response curves were used to calculate EC_{50} values for the compounds. Shown are
581 representative dose-response curves converted to percentage from one of three
582 independent experiments. For EC_{50} values of all experiments, see Supp. Figure 1. Difference
583 in EC_{50} values between the strains were determined not to be significant using a Kruskal-
584 Wallis one-way analysis of variance.
585
586 **Figure 3. Dose-response curve of *P. knowlesi* cultured in the presence of ML10 and effect**
587 **of serum on EC_{50} of ML10.**
588 Dose-response curves derived from parasite growth inhibition assays obtained with *P.*
589 *knowlesi* (**A**) and *P. falciparum* strain 3D7 cultured in RPMI-1640 with or without
590 supplementation with 10% horse serum (**B**). These results were used to calculate the EC_{50} of
591 ML10 on parasites during the erythrocytic stage. (**C**) Effect of 150 nM ML10 on the growth
592 of *P. knowlesi* egress. Late stage synchronized parasites were incubated in the presence of
593 150 nM ML10 (bars on left-hand and right-hand side) or DMSO (bars in middle). When ring-
594 stage parasites were detected in the untreated sample (approximately 2 h after addition of
595 ML10), the parasites were washed to remove the ML10 or DMSO. Parasites were
596 subsequently incubated in the presence of DMSO or ML10. Note that 150 mM ML10
597 completely blocks progression to the next cycle, whereas removal of the compound after
598 two hours of incubation has no effect on the parasitemia in the next cycle. Results of
599 statistical comparison of the ML10-treated sample with the DMSO and the wash-out sample
600 in each cycle are indicated: no symbol: no significant difference; *: $p \leq 0.05$; **: $p \leq 0.01$. (**D**,
601 **E**) To identify an effective working concentration of ML10 for *P. falciparum* in the presence
602 of serum, parasite cultures were cultured in the presence of 0.5% AlbuMax alone or
603 AlbuMax and 5% serum (**E**) or 10% serum (without additional AlbuMax) (**F**) and ML10 at
604 concentrations ranging from 0-75 nM for one cycle. Start (black bars) denotes the
605 parasitemia of the culture in the first cycle, prior to the addition of ML10. Error bars denote
606 the standard deviation of three replicates. Results of statistical comparison of 0 nM sample
607 with the samples treated with ML10 is indicated: *: $p \leq 0.05$; ***$p \leq 0.001$.
608

609 **Figure 4. Impact of the length of exposure of arrested mature schizonts to ML10 or**
610 **Compound 2 on parasite viability.** (**A**) Cultures containing mature schizonts were
611 maintained for 0-12 hours in either DMSO, 25 nM ML10 or 1.5 µM Compound 2 and
612 subsequently washed and allowed to egress and invade fresh red blood cells. The resulting
613 parasitemia was determined by flow cytometry and reflects the survival of the parasites in
614 the compound. Shown is a representative experiment of five independent experiments;
615 each experiment consisted of three technical replicates. The statistical significance of the
616 difference between the parasitemia of the culture treated for one hour and the subsequent
617 samples was determined using an unpaired t-test; ** = $p \leq 0.01$, *** = $p \leq 0.001$, whereas no
618 symbol indicates no statistical significance. (**B**) Giemsa-stained parasite smears were
619 produced immediately prior to removal of the compound to ascertain the effect of
620 incubation in the presence of the compound on the morphology of the parasites. Numbers
621 above the images denote the length of time (in hours) the parasites had been exposed to
622 the compound.
623
624 **Figure 5. Synchronicity of invasion after removal of inhibition by ML10 or Compound 2.**
625 (**A**) Parasites that had been arrested with either ML10 (blue bars) or Compound 2 (grey
626 bars) for up to three hours were washed to allow egress and invasion of new erythrocytes.
627 Samples were removed at 10-minute intervals and the percentage of host cells infected with
628 ring forms, which represent parasites that have egressed and invaded new erythrocytes,
629 was determined by cytometry (see Supp. Figure 3 for gating strategy). Error bars represent
630 standard deviation from 3 independent experiments each conducted in duplicate, no
631 statistically significant differences were detected between compounds at each time point
632 using a pairwise individual t-test. (**B)** Giemsa smears made at the time point indicated at the
633 top confirmed the presence of ring-stage parasites in the samples.
634
635 **Figure 6. Growth of *P. falciparum* in the presence of ML10**.
636 (**A**) Cultures of *P. falciparum* strain 3D7 consisting of rings no older than 2 hours were
637 treated with 25 nM ML10 or an equivalent amount of DMSO and parasite development was
638 monitored throughout the erythrocytic cycle for the synthesis of DNA, as measured by SYBR
639 Green I staining and flow cytometry (top panels; gold represents the DMSO-treated sample,
640 while blue represents the ML-10 treated sample. The number in each panel indicates hours
641 after onset of invasion, while the x-axis shows the nucleic acid content as measured with
642 SYBR Green I staining) and imagining of Giemsa-stained smears (bottom panels). At the 47-
643 hour time point (three hours after ring-stage parasites were first detected in the DMSO-
644 treated samples), DMSO and ML10 were removed. (**B**) The parasitemia of the cultures in (A)
645 was determined at each time point. Note the similar parasitemias of the DMSO-treated and
646 ML10-treated samples in the second cycle, indicating that the presence of ML10 in the first
647 cycle did not affect the development of the parasites. The cultures were set up in triplicate,
648 error bars represent standard deviation at each time point. The statistical significance of the
649 difference between the parasitemia of the DMSO-treated and ML10-treated samples at
650 each time point was calculated using an unpaired t-test; *** indicates $p \leq 0.001$, whereas no
651 symbol indicates no statistical significance. (**C**) Growth of *P. falciparum* strains 3D7 and
652 T618Q over four cycles. Parasite cultures were diluted to a parasitemia of ~0.1% and growth
653 was monitored over four cycles. Medium was changed daily after four days. Note the nearly
654 identical growth of the DMSO-treated and ML10-treated T618Q parasites. The cultures
655 were set up in triplicate, error bars represent standard deviation at each time point. The

656 statistical significance of the difference between the parasitemia of the DMSO-treated and
657 ML10-treated samples for each strain at each cycle was calculated using an unpaired t-test;
658 *= $p \leq 0.05$ and ***=$p \leq 0.001$, whereas no symbol indicates no statistical significance. The
659 graphs represent one of three biological replicates.
660
661 **Supplementary Figure 1. Scatter plots of the mean EC_{50} values obtained from multiple**
662 **independent dose-response curves with different *P. falciparum* lines and culture**
663 **conditions and *P. knowlesi*.** Mean EC_{50} values for *P. falciparum* strains 3D7, Dd2, HB3 and
664 NF54 grown in standard culture conditions (0.5% AlbuMax) in the presence of ML10 (**A**) or
665 Compound 2 (**B**). (**C**) Mean EC_{50} values obtained with *P. falciparum* strain 3D7 grown in
666 standard culture conditions (0.5% AlbuMax) or in RPMI-1640 containing 0.5% AlbuMax and
667 10% horse serum. (**D**) Mean EC_{50} values obtained with *P. knowlesi* strain A1-H.1 grown in
668 standard culture conditions using RPMI-1640 containing 0.5% AlbuMax and 10% horse
669 serum. Error bars are standard deviation of the calculated means.
670
671 **Supplementary Figure 2. Pairwise scatter plots depicting the start and duration of egress**
672 **after removal of ML10 or Compound 2**
673 Quantification of the period until the first schizont egress event was detected (**A**) and time
674 required for egress of the majority of schizonts after egression of the first schizont (**B**).
675 Values were attained from the analysis of egress videos after removal of ML10 or
676 Compound 2 from 3 independent experiments. No significant differences were detected
677 using a paired t-test.
678
679 **Supplementary Figure 3. Gating strategy for determination of rings after compound**
680 **washout represented in Figure 5.** Representative gating strategies for the determination of
681 parasitized erythrocytes stained with SYBR Green I nuclear staining and their respective ring
682 and schizont stage, 10 minutes (**A**) and 60 minutes after (**B**) compound washout. (**C**) Overlay
683 of histograms of the two time points emphasizing the differences in signal profiles between
684 ring and schizont populations.
685
686 **Supplementary Video 1. Video microscopy of egress after removal of ML10**
687 Egress of *P. falciparum* merozoites *in vitro* imaged by time-lapse video microscopy following
688 removal of ML10.
689
690 **Supplementary Video 2. Video microscopy of egress after removal of Compound 2**
691 Egress of *P. falciparum* merozoites *in vitro* imaged by time-lapse video microscopy following
692 removal of Compound 2**.**
693
694
695
696

697 **REFERENCES**
698
699

700 1. Bozdech Z, Llinas M, Pulliam BL, Wong ED, Zhu J, DeRisi JL. The transcriptome of the
701 intraerythrocytic developmental cycle of *Plasmodium falciparum*. *PLoS Biol*. 2003;1(1):E5.
702 2. Le Roch KG, Zhou Y, Blair PL, Grainger M, Moch JK, Haynes JD, et al. Discovery of
703 gene function by expression profiling of the malaria parasite life cycle. *Science*.
704 2003;301(5639):1503-8.
705 3. Llinas M, Bozdech Z, Wong ED, Adai AT, DeRisi JL. Comparative whole genome
706 transcriptome analysis of three *Plasmodium falciparum* strains. *Nucleic Acids Res*.
707 2006;34(4):1166-73.
708 4. Chua ACY, Ong JJY, Malleret B, Suwanarusk R, Kosaisavee V, Zeeman AM, et al.
709 Robust continuous *in vitro* culture of the *Plasmodium cynomolgi* erythrocytic stages. *Nat*
710 *Commun.* 2019;10(1):3635.
711 5. Lim C, Hansen E, DeSimone TM, Moreno Y, Junker K, Bei A, et al. Expansion of host
712 cellular niche can drive adaptation of a zoonotic malaria parasite to humans. *Nat Commun*.
713 2013;4:1638.
714 6. Moon RW, Hall J, Rangkuti F, Ho YS, Almond N, Mitchell GH, et al. Adaptation of the
715 genetically tractable malaria pathogen *Plasmodium knowlesi* to continuous culture in
716 human erythrocytes. *Proc Natl Acad Sci U S A*. 2013;110(2):531-6.
717 7. Trager W, Jensen JB. Human malaria parasites in continuous culture. *Science*.
718 1976;193(4254):673-5.
719 8. Hirako IC, Assis PA, Hojo-Souza NS, Reed G, Nakaya H, Golenbock DT, et al. Daily
720 Rhythms of TNFalpha Expression and Food Intake Regulate Synchrony of *Plasmodium* Stages
721 with the Host Circadian Cycle. *Cell Host Microbe*. 2018;23(6):796-808 e6.
722 9. Mideo N, Reece SE, Smith AL, Metcalf CJ. The Cinderella syndrome: why do malaria-
723 infected cells burst at midnight? *Trends Parasitol*. 2013;29(1):10-6.
724 10. Kwiatkowski D, Greenwood BM. Why is malaria fever periodic? A hypothesis.
725 *Parasitol Today*. 1989;5(8):264-6.
726 11. O'Donnell AJ, Schneider P, McWatters HG, Reece SE. Fitness costs of disrupting
727 circadian rhythms in malaria parasites. *Proc Biol Sci*. 2011;278(1717):2429-36.
728 12. Glushakova S, Beck JR, Garten M, Busse BL, Nasamu AS, Tenkova-Heuser T, et al.
729 Rounding precedes rupture and breakdown of vacuolar membranes minutes before malaria
730 parasite egress from erythrocytes. *Cell Microbiol*. 2018;20(10):e12868.
731 13. Hale VL, Watermeyer JM, Hackett F, Vizcay-Barrena G, van Ooij C, Thomas JA, et al.
732 Parasitophorous vacuole poration precedes its rupture and rapid host erythrocyte
733 cytoskeleton collapse in *Plasmodium falciparum* egress. *Proc Natl Acad Sci U S A*.
734 2017;114(13):3439-44.
735 14. Thomas JA, Tan MSY, Bisson C, Borg A, Umrekar TR, Hackett F, et al. A protease
736 cascade regulates release of the human malaria parasite *Plasmodium falciparum* from host
737 red blood cells. *Nat Microbiol*. 2018;3(4):447-55.
738 15. Weiss GE, Gilson PR, Taechalertpaisarn T, Tham WH, de Jong NW, Harvey KL, et al.
739 Revealing the sequence and resulting cellular morphology of receptor-ligand interactions
740 during *Plasmodium falciparum* invasion of erythrocytes. *PLoS Pathog*. 2015;11(2):e1004670.
741 16. Inselburg J, Banyal HS. *Plasmodium falciparum*: synchronization of asexual
742 development with aphidicolin, a DNA synthesis inhibitor. Exp Parasitol. 1984;57(1):48-54.

743 17. Assaraf YG, Golenser J, Spira DT, Bachrach U. *Plasmodium falciparum*:
744 synchronization of cultures with DL-alpha-difluoromethylornithine, an inhibitor of
745 polyamine biosynthesis. *Exp Parasitol*. 1986;61(2):229-35.
746 18. van Biljon R, Niemand J, van Wyk R, Clark K, Verlinden B, Abrie C, et al. Inducing
747 controlled cell cycle arrest and re-entry during asexual proliferation of *Plasmodium*
748 *falciparum* malaria parasites. *Sci Rep*. 2018;8(1):16581.
749 19. Lambros C, Vanderberg JP. Synchronization of *Plasmodium falciparum* erythrocytic
750 stages in culture. *J Parasitol*. 1979;65(3):418-20.
751 20. Ngernna S, Chim-Ong A, Roobsoong W, Sattabongkot J, Cui L, Nguitragool W.
752 Efficient synchronization of *Plasmodium knowlesi in vitro* cultures using guanidine
753 hydrochloride. Malar J. 2019;18(1):148.
754 21. Brown AC, Moore CC, Guler JL. Cholesterol-dependent enrichment of understudied
755 erythrocytic stages of human *Plasmodium parasites*. *Sci Rep*. 2020;10(1):4591.
756 22. Geislinger TM, Chan S, Moll K, Wixforth A, Wahlgren M, Franke T. Label-free
757 microfluidic enrichment of ring-stage *Plasmodium falciparum*-infected red blood cells using
758 non-inertial hydrodynamic lift. *Malar J*. 2014;13:375.
759 23. Tosta CE, Sedegah M, Henderson DC, Wedderburn N. *Plasmodium yoelii* and
760 *Plasmodium berghei*: isolation of infected erythrocytes from blood by colloidal silica
761 gradient centrifugation. *Exp Parasitol*. 1980;50(1):7-15.
762 24. Saul A, Myler P, Elliott T, Kidson C. Purification of mature schizonts of *Plasmodium*
763 *falciparum* on colloidal silica gradients. *Bull World Health Organ*. 1982;60(5):755-9.
764 25. Rivadeneira EM, Wasserman M, Espinal CT. Separation and concentration of
765 schizonts of *Plasmodium falciparum* by Percoll gradients. *J Protozool*. 1983;30(2):367-70.
766 26. Kramer KJ, Kan SC, Siddiqui WA. Concentration of *Plasmodium falciparum*-infected
767 erythrocytes by density gradient centrifugation in Percoll. *J Parasitol*. 1982;68(2):336-7.
768 27. Radfar A, Mendez D, Moneriz C, Linares M, Marin-Garcia P, Puyet A, et al.
769 Synchronous culture of *Plasmodium falciparum* at high parasitemia levels. *Nat Protoc*.
770 2009;4(12):1899-915.
771 28. Childs RA, Miao J, Gowda C, Cui L. An alternative protocol for *Plasmodium falciparum*
772 culture synchronization and a new method for synchrony confirmation. *Malar J*.
773 2013;12:386.
774 29. Mata-Cantero L, Lafuente MJ, Sanz L, Rodriguez MS. Magnetic isolation of
775 *Plasmodium falciparum* schizonts iRBCs to generate a high parasitaemia and synchronized *in*
776 *vitro* culture. *Malar J.* 2014;13:112.
777 30. Trang DT, Huy NT, Kariu T, Tajima K, Kamei K. One-step concentration of malarial
778 parasite-infected red blood cells and removal of contaminating white blood cells. *Malar J.*
779 2004;3:7.
780 31. Paul F, Roath S, Melville D, Warhurst DC, Osisanya JO. Separation of malaria-infected
781 erythrocytes from whole blood: use of a selective high-gradient magnetic separation
782 technique. *Lancet*. 1981;2(8237):70-1.
783 32. Ranford-Cartwright LC, Sinha A, Humphreys GS, Mwangi JM. New synchronization
784 method for *Plasmodium falciparum*. *Malar J*. 2010;9:170.
785 33. Boyle MJ, Wilson DW, Richards JS, Riglar DT, Tetteh KK, Conway DJ, et al. Isolation of
786 viable *Plasmodium falciparum* merozoites to define erythrocyte invasion events and
787 advance vaccine and drug development. *Proc Natl Acad Sci U S A*. 2010;107(32):14378-83.
788 Epub 2010/07/28.

789 34. Lyth O, Vizcay-Barrena G, Wright KE, Haase S, Mohring F, Najer A, et al. Cellular
790 dissection of malaria parasite invasion of human erythrocytes using viable *Plasmodium*
791 *knowlesi* merozoites. Sci Rep. 2018;8(1):10165.
792 35. Dennis ED, Mitchell GH, Butcher GA, Cohen S. *In vitro* isolation of *Plasmodium*
793 *knowlesi* merozoites using polycarbonate sieves. *Parasitology*. 1975;71(3):475-81.
794 36. Knuepfer E, Suleyman O, Dluzewski AR, Straschil U, O'Keeffe AH, Ogun SA, et al.
795 RON12, a novel *Plasmodium*-specific rhoptry neck protein important for parasite
796 proliferation. *Cell Microbiol*. 2014;16(5):657-72.
797 37. Alam MM, Solyakov L, Bottrill AR, Flueck C, Siddiqui FA, Singh S, et al.
798 Phosphoproteomics reveals malaria parasite Protein Kinase G as a signalling hub regulating
799 egress and invasion. *Nat Commun*. 2015;6:7285.
800 38. Collins CR, Hackett F, Strath M, Penzo M, Withers-Martinez C, Baker DA, et al.
801 Malaria parasite cGMP-dependent protein kinase regulates blood stage merozoite secretory
802 organelle discharge and egress. *PLoS Pathog*. 2013;9(5):e1003344.
803 39. Diaz CA, Allocco J, Powles MA, Yeung L, Donald RG, Anderson JW, et al.
804 Characterization of *Plasmodium falciparum* cGMP-dependent protein kinase (PfPKG):
805 antiparasitic activity of a PKG inhibitor. *Mol Biochem Parasitol*. 2006;146(1):78-88.
806 40. Taylor HM, McRobert L, Grainger M, Sicard A, Dluzewski AR, Hopp CS, et al. The
807 malaria parasite cyclic GMP-dependent protein kinase plays a central role in blood-stage
808 schizogony. *Eukaryot Cell*. 2010;9(1):37-45.
809 41. Donald RG, Zhong T, Wiersma H, Nare B, Yao D, Lee A, et al. Anticoccidial kinase
810 inhibitors: identification of protein kinase targets secondary to cGMP-dependent protein
811 kinase. *Mol Biochem Parasitol*. 2006;149(1):86-98.
812 42. Collins CR, Hackett F, Atid J, Tan MSY, Blackman MJ. The *Plasmodium falciparum*
813 pseudoprotease SERA5 regulates the kinetics and efficiency of malaria parasite egress from
814 host erythrocytes. *PLoS Pathog*. 2017;13(7):e1006453.
815 43. Sherling ES, Knuepfer E, Brzostowski JA, Miller LH, Blackman MJ, van Ooij C. The
816 *Plasmodium falciparum* rhoptry protein RhopH3 plays essential roles in host cell invasion
817 and nutrient uptake. Elife. 2017;6.
818 44. Mohring F, Hart MN, Rawlinson TA, Henrici R, Charleston JA, Diez Benavente E, et al.
819 Rapid and iterative genome editing in the malaria parasite *Plasmodium knowlesi* provides
820 new tools for *P. vivax* research. Elife. 2019;8.
821 45. Pino P, Caldelari R, Mukherjee B, Vahokoski J, Klages N, Maco B, et al. A multistage
822 antimalarial targets the plasmepsins IX and X essential for invasion and egress. *Science*.
823 2017;358(6362):522-8.
824 46. Baker DA, Stewart LB, Large JM, Bowyer PW, Ansell KH, Jimenez-Diaz MB, et al. A
825 potent series targeting the malarial cGMP-dependent protein kinase clears infection and
826 blocks transmission. *Nat Commun*. 2017;8(1):430.
827 47. Smilkstein M, Sriwilaijaroen N, Kelly JX, Wilairat P, Riscoe M. Simple and inexpensive
828 fluorescence-based technique for high-throughput antimalarial drug screening. *Antimicrob*
829 *Agents Chemother.* 2004;48(5):1803-6.
830 48. Gurnett AM, Liberator PA, Dulski PM, Salowe SP, Donald RG, Anderson JW, et al.
831 Purification and molecular characterization of cGMP-dependent protein kinase from
832 Apicomplexan parasites. A novel chemotherapeutic target. *J Biol Chem*.
833 2002;277(18):15913-22.
834 49. Chugh M, Scheurer C, Sax S, Bilsland E, van Schalkwyk DA, Wicht KJ, et al.
835 Identification and deconvolution of cross-resistance signals from antimalarial compounds

836 using multidrug-resistant *Plasmodium falciparum* strains. *Antimicrob Agents Chemother*.
837 2015;59(2):1110-8.
838 50. Murray L, Stewart LB, Tarr SJ, Ahouidi AD, Diakite M, Amambua-Ngwa A, et al.
839 Multiplication rate variation in the human malaria parasite *Plasmodium falciparum*. *Sci Rep*.
840 2017;7(1):6436.
841 51. van Schalkwyk DA, Moon RW, Blasco B, Sutherland CJ. Comparison of the
842 susceptibility of *Plasmodium knowlesi* and *Plasmodium falciparum* to antimalarial agents. J
843 *Antimicrob Chemother*. 2017;72(11):3051-8.
844 52. van Schalkwyk DA, Blasco B, Davina Nunez R, Liew JWK, Amir A, Lau YL, et al.
845 *Plasmodium knowlesi* exhibits distinct in vitro drug susceptibility profiles from those of
846 *Plasmodium falciparum*. *Int J Parasitol Drugs Drug Resist*. 2019;9:93-9.
847 53. Boyle MJ, Richards JS, Gilson PR, Chai W, Beeson JG. Interactions with heparin-like
848 molecules during erythrocyte invasion by *Plasmodium falciparum* merozoites. Blood.
849 2010;115(22):4559-68.
850 54. Das S, Hertrich N, Perrin AJ, Withers-Martinez C, Collins CR, Jones ML, et al.
851 Processing of *Plasmodium falciparum* Merozoite Surface Protein MSP1 Activates a Spectrin-
852 Binding Function Enabling Parasite Egress from RBCs. *Cell Host Microbe*. 2015;18(4):433-44.
853 Epub 2015/10/16.
854 55. Patel A, Perrin AJ, Flynn HR, Bisson C, Withers-Martinez C, Treeck M, et al. Cyclic
855 AMP signalling controls key components of malaria parasite host cell invasion machinery.
856 *PLoS Biol*. 2019;17(5):e3000264.
857 56. Flueck C, Drought LG, Jones A, Patel A, Perrin AJ, Walker EM, et al.
858 Phosphodiesterase beta is the master regulator of cAMP signalling during malaria parasite
859 invasion. *PLoS Biol*. 2019;17(2):e3000154. Epub 2019/02/23.
860 57. Bannister LH, Hopkins JM, Margos G, Dluzewski AR, Mitchell GH. Three-dimensional
861 ultrastructure of the ring stage of *Plasmodium falciparum*: evidence for export pathways.
862 *Microsc Microanal*. 2004;10(5):551-62.
863 58. Gruring C, Heiber A, Kruse F, Ungefehr J, Gilberger TW, Spielmann T. Development
864 and host cell modifications of *Plasmodium falciparum* blood stages in four dimensions. *Nat*
865 *Commun*. 2011;2:165.
866 59. Collins CR, Das S, Wong EH, Andenmatten N, Stallmach R, Hackett F, et al. Robust
867 inducible Cre recombinase activity in the human malaria parasite *Plasmodium falciparum*
868 enables efficient gene deletion within a single asexual erythrocytic growth cycle. *Mol*
869 *Microbiol.* 2013;88(4):687-701.
870 60. Portugaliza HP, Llora-Batlle O, Rosanas-Urgell A, Cortes A. Reporter lines based on
871 the *gexp02* promoter enable early quantification of sexual conversion rates in the malaria
872 parasite *Plasmodium falciparum*. *Sci Rep*. 2019;9(1):14595.
873 61. Perrin AJ, Collins CR, Russell MRG, Collinson LM, Baker DA, Blackman MJ. The
874 Actinomyosin Motor Drives Malaria Parasite Red Blood Cell Invasion but Not Egress. *MBio*.
875 2018;9(4).
876 62. Chang CY, Simon E. The effect of dimethyl sulfoxide (DMSO) on cellular systems. *Proc*
877 *Soc Exp Biol Med.* 1968;128(1):60-6.
878 63. Lampugnani MG, Pedenovi M, Niewiarowski A, Casali B, Donati MB, Corbascio GC, et
879 al. Effects of dimethyl sulfoxide (DMSO) on microfilament organization, cellular adhesion,
880 and growth of cultured mouse B16 melanoma cells. *Exp Cell Res*. 1987;172(2):385-96.

881 64. Moon RW, Sharaf H, Hastings CH, Ho YS, Nair MB, Rchiad Z, et al. Normocyte-binding
882 protein required for human erythrocyte invasion by the zoonotic malaria parasite
883 *Plasmodium knowlesi*. Proc Natl Acad Sci U S A. 2016;113(26):7231-6.
884
885

Figure 1

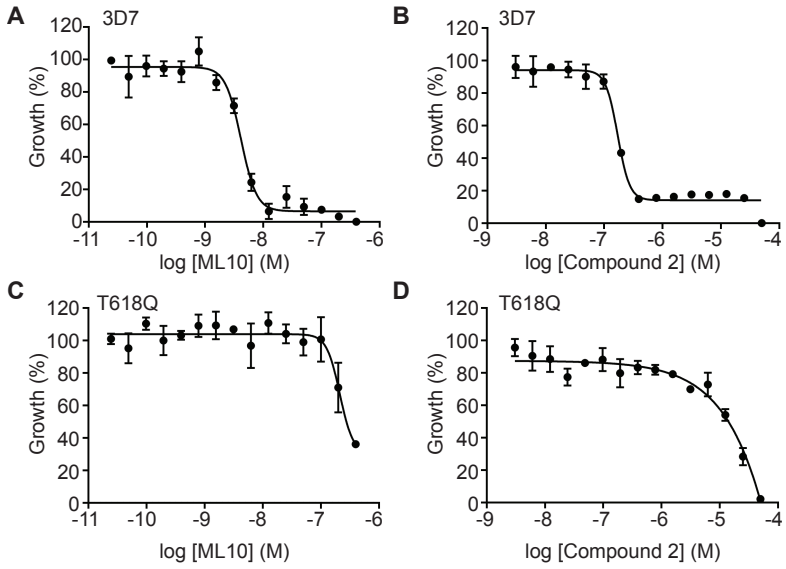
A
3D7
Growth (%)
log [ML10] (M)
B
3D7
Growth (%)
log [Compound 2] (M)
C
T618Q
Growth (%)
log [ML10] (M)
D
T618Q
Growth (%)
log [Compound 2] (M)

886

Figure 2

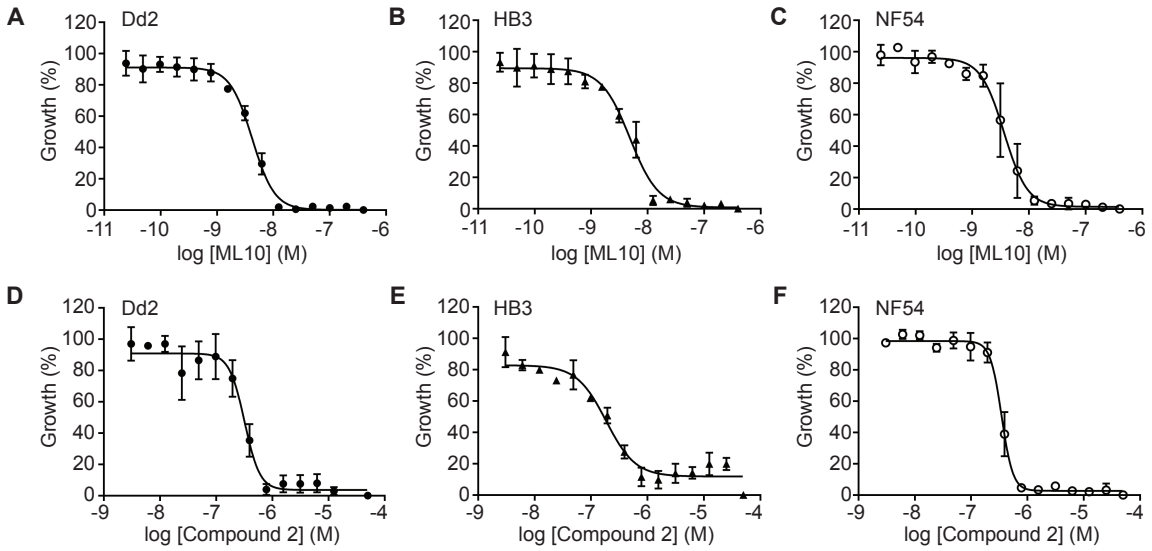
A
Dd2
B
HB3
C
NF54
D
Dd2
E
HB3
F
NF54
Growth (%)
log [ML10] (M)
log [Compound 2] (M)

887

Figure 3

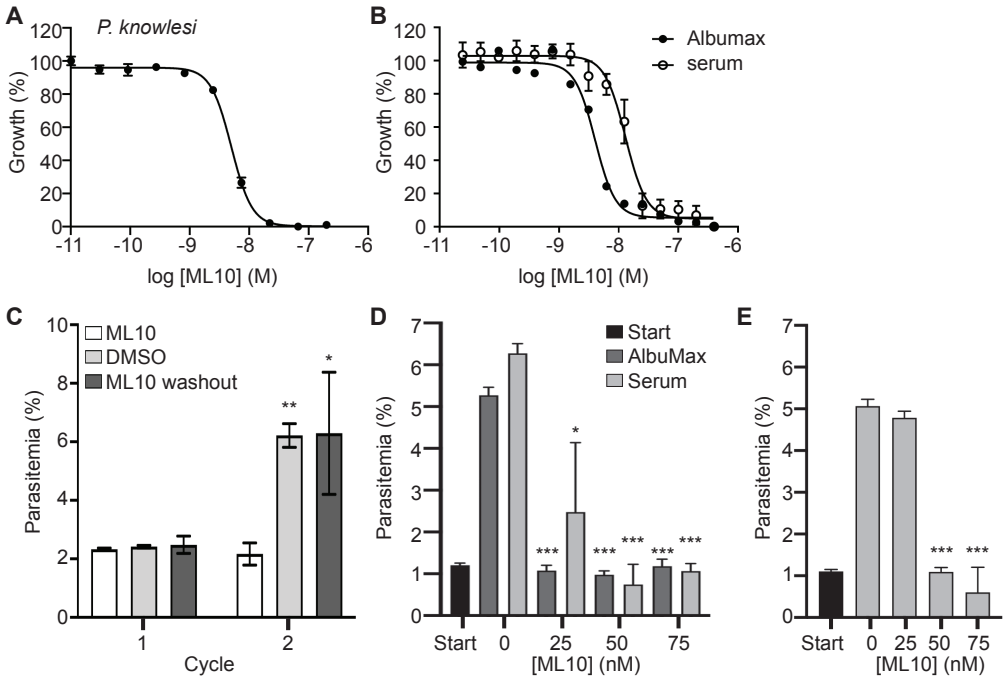
A
P. knowlesi
Growth (%)
log [ML10] (M)
B
Albumax
serum
Growth (%)
log [ML10] (M)
C
ML10
DMSO
ML10 washout
Parasitemia (%)
Cycle
D
Start
AlbuMax
Serum
Parasitemia (%)
[ML10] (nM)
E
Parasitemia (%)
[ML10] (nM)

888

Figure 4

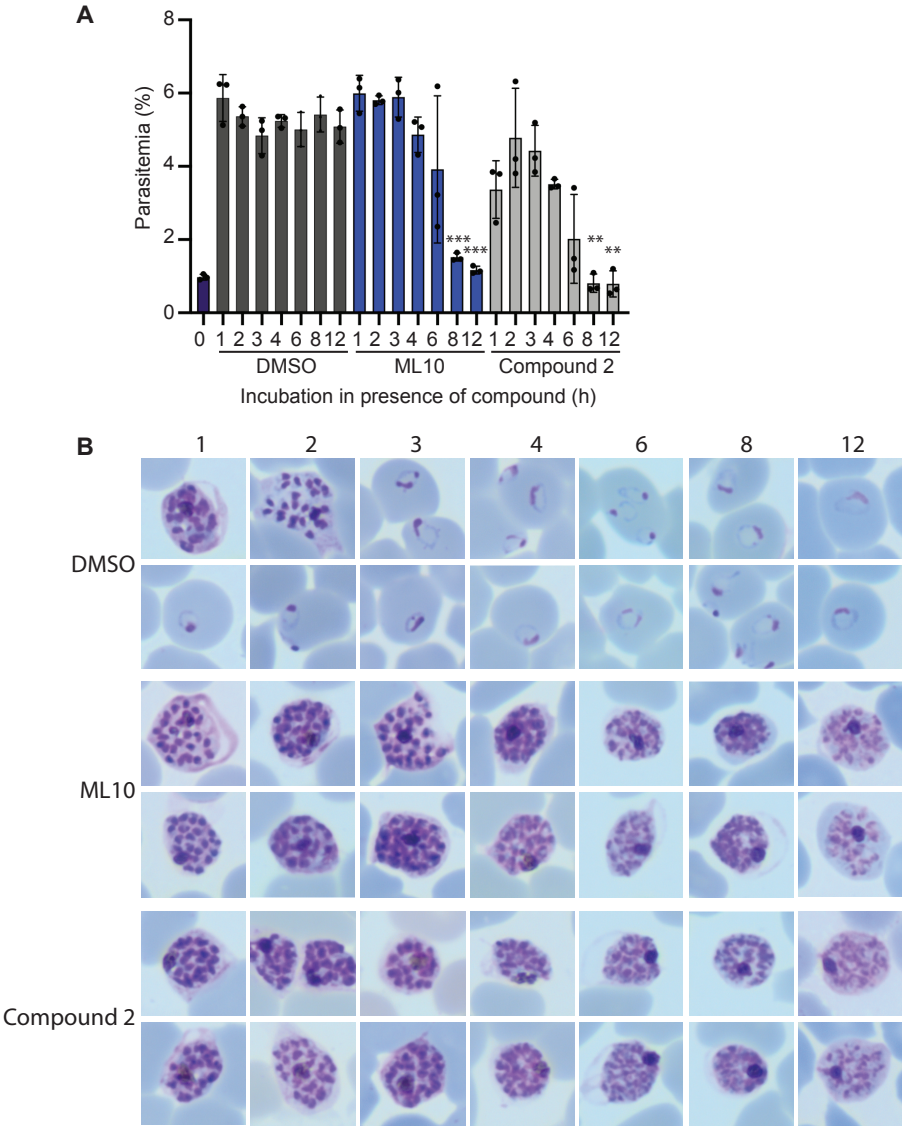
A
Parasitemia (%)
8
6
4
2
0
0 1 2 3 4 6 8 12 1 2 3 4 6 8 12 1 2 3 4 6 8 12
DMSO
ML10
Compound 2
Incubation in presence of compound (h)
***
***
**
**
B
1
2
3
4
6
8
12
DMSO
ML10
Compound 2

889

Figure 5

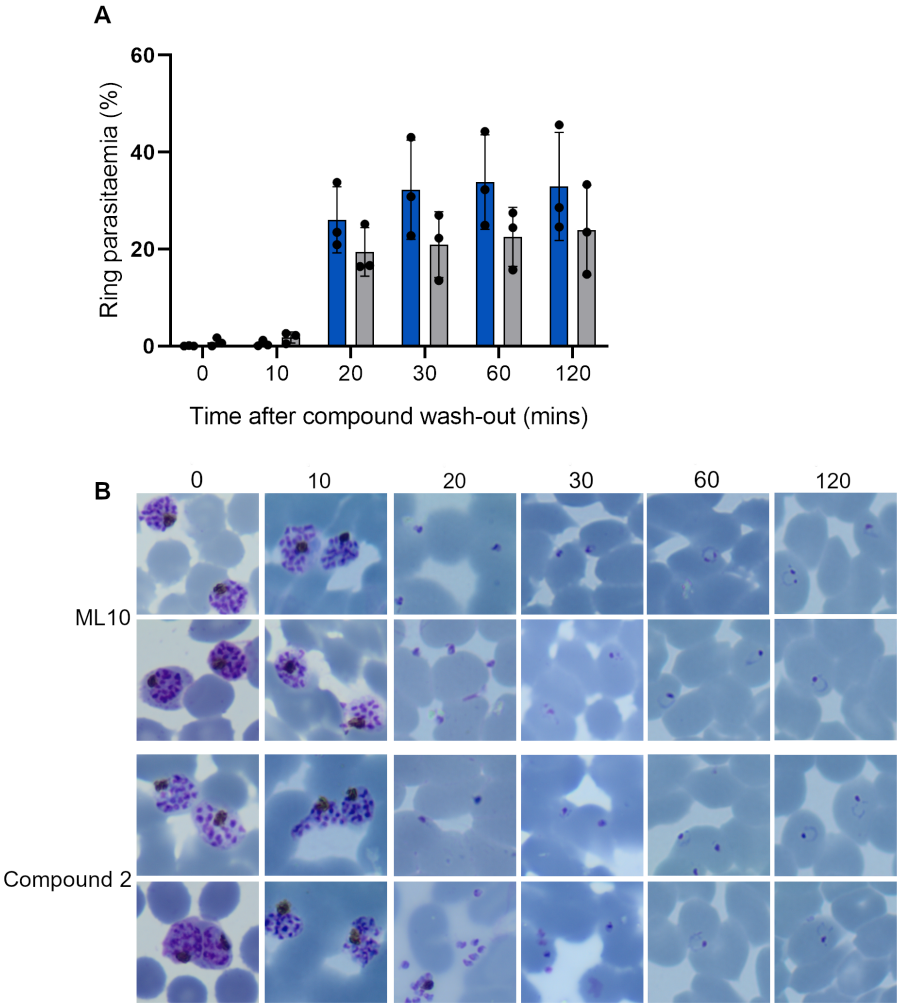
A
Ring parasitaemia (%)
60
40
20
0
0
10
20
30
60
120
Time after compound wash-out (mins)
B
0
10
20
30
60
120
ML10
Compound 2

890

Figure 6

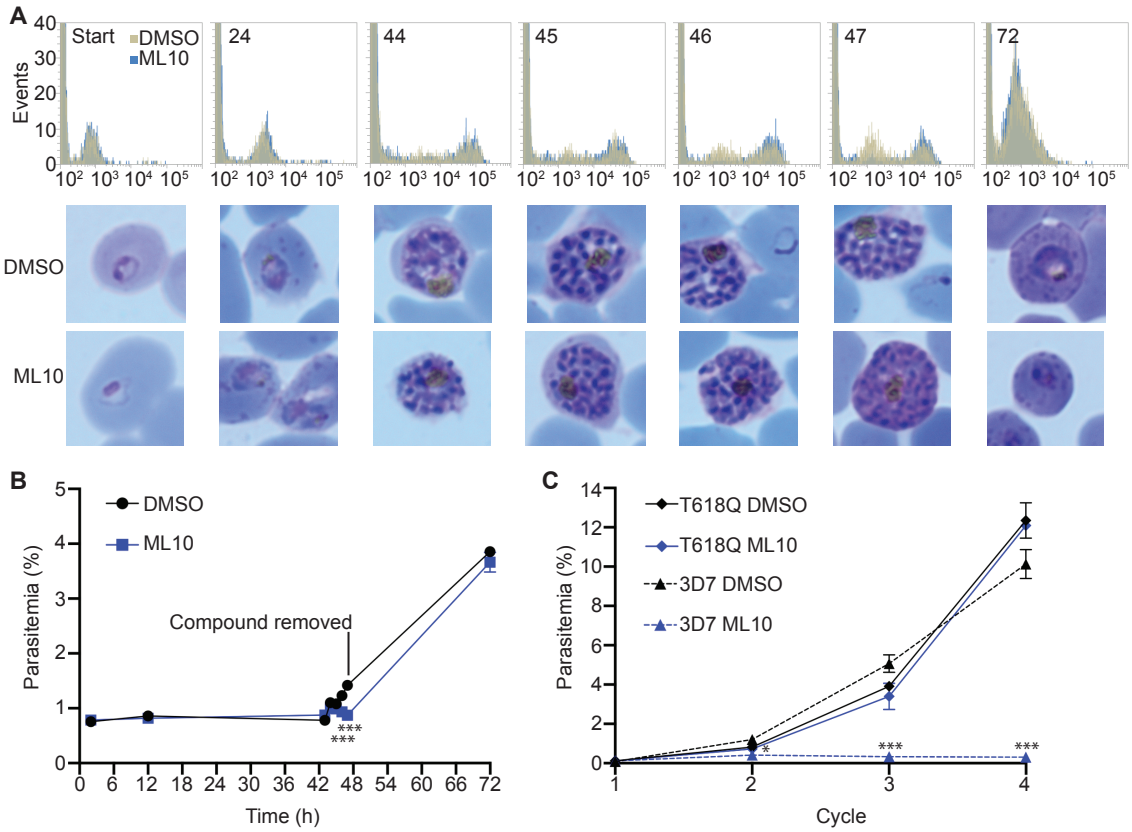
A
Start
DMSO
ML10
24
44
45
46
47
72
Events
DMSO
ML10
B
DMSO
ML10
Compound removed
Parasitemia (%)
Time (h)
C
T618Q DMSO
T618Q ML10
3D7 DMSO
3D7 ML10
Parasitemia (%)
Cycle

891